PHYSICAL REVIEW B VOLUME 34, NUMBER 8 15 OCTOBER 1986

Optical constants of palladium silicides measured by a multiple-wavelength ellipsometer

Juh Tzeng Lue
Department of Physics, National Tsing Hua University, Hsinchu, Taiwan, Republic of China

Hong-Wen Chen
Department of Electrical Engineering, National Tsing Hua University, Hsinchu, Taiwan, Republic of China

Shwa-Ing Lew
Department of Physics, National Tsing Hua University, Hsinchu, Taiwan, Republic of China
(Received 18 December 1985)

The optical absorption and dispersion of as-deposited Pd, Pd_2Si, and PdSi are measured by an ellipsometer at wavelengths of 400 to 700 nm. The imaginary part of the refractive index is shown to decrease by a value of 4 from the as-deposited Pd to the high-temperature annealed PdSi. The binding energy of the Pd $3d_{5/2}$ core electrons shifts by 1.8 ± 0.2 eV as studied by x-ray photoelectron spectroscopy.

I. INTRODUCTION

Though palladium silicides have long been used in optoelectronic devices such as in buffering layers for preventing the interdiffusion of silicon and other metals,[1] or in the Schottky-barrier contact of infrared image sensors,[2] few of their optical and electronic properties are reported.[3] A study of their electronic bond structures and refractive indices is important to devise fabrication. Silicides grown at high temperatures are usually accompanied by a thin oxide layer on the surface. Direct determination of optical constant by the absolute reflectivity method[4] usually introduces catastrophic errors. In the present study, a multiple-wavelength ellipsometer is constructed to detect optical constants of multiple layers. The chemical composition and depth profile of palladium silicides formed at different annealing temperatures are examined by an Auger-electron spectrometer (AES). The silicides are determined to be Pd_2Si and PdSi, respectively, for annealing at temperatures of 400 and 800 °C, respectively, with a duration of 40 min. The electronic binding energy of Pd $3d_{5/2}$ measured by an x-ray photoelectron spectrometer (XPS) increases as the annealing temperature increases. This means a loss of electrons from the Pd valence shell in forming the silicide complexes. The refractive indices change drastically in response to different electronic structures.

II. ELLIPSOMETRY STUDY

Ellipsometry is the measurement of the effect of reflections on the s and p polarization states of incident light. The extinction ratio of the reflected p and s waves can be derived from the Fresnel reflection coefficients and is given by[5]

$$\rho=\frac{|R_p|}{|R_s|}e^{i(\delta_p-\delta_s)}=\tan\psi\, e^{i\Delta}\ , \tag{1}$$

where ψ is the arctangent of the ratio of the amplitudes of the R_p and R_s reflecting waves, and Δ is the difference between the phase shift of the reflecting p and s waves. If the compensator is a quarter-wave plate, the relationships between Δ and ψ, then the extinction settings are simply given by

$$\Delta=90^\circ-2P_0,\quad \psi=-A_0\ , \tag{2}$$

where P_0 and A_0 are the polarizer and analyzer extinction settings, respectively. For a simple bulk substrate, the complex refractive index N_1 of the substrate can be readily derived from the value of ρ by exploiting the following equation:

$$N_1=n_0\tan\phi_0\left[1-\frac{4\rho}{(1+\rho)^2}\sin^2\phi_0\right]^{1/2}\ , \tag{3}$$

where n_0 is the refractive index of the ambient and ϕ_0 is the incident angle. In the silicide system, multiple reflections between interfacial layers of air to silicide (with subindices of 0 to 1), silicide to substrate (1 to 2), and silicide back to air (1 to 0) occur, therefore the total reflection is

$$\begin{aligned} R&=r_{01}+t_{12}e^{2i\beta}+t_{01}t_{10}r_{12}^2e^{-4i\beta}\\ &\quad+t_{01}t_{10}r_{10}^2r_{12}^2e^{-6i\beta}+\cdots\\ &=\frac{r_{01}+r_{12}e^{2i\beta}}{1+r_{01}r_{12}e^{-2i\beta}}\ , \end{aligned} \tag{4}$$

where r_{nm} and t_{nm} are the Fresnel reflection and transmission coefficients, respectively, from medium n to medium m, and β is the phase shift through the silicide thickness d which is written as

$$\beta=2\pi\left[\frac{d_1}{\lambda}\right]N_1\cos\phi_1\ , \tag{5}$$

where ϕ_1 is the angle of refraction. If the reflectance R is

 ©1986 The American Physical Society

decomposed into p and s polarized waves, the ellipsometry function becomes

$$\rho=\tan\psi\, e^{i\Delta}=\frac{R_p}{R_s}=\frac{r_{01}^p+r_{12}^p e^{-2i\beta}}{1+r_{01}^p e^{-2i\beta}}\,\frac{1+r_{01}^s r_{12}^s e^{-2i\beta}}{r_{01}^s+r_{12}^s e^{-2i\beta}}$$

$$=\rho(N_0,N_1,N_2,d_1,\phi_0,\lambda)\ . \qquad (6)$$

For an absorbing silicide film, $N_1=n_1-ik_1$, we need multiple incident angles to solve the unknown parameters from sets of equations. Each refractive angle ϕ_i can give one pair of $\Delta_i(B,\phi_i)$ and $\psi_i(B,\phi_i)$. The parameters B with a component b_j denoting one of the N_0, N_1, N_2, d_1, and ϕ can be numerically solved from an elaborate mean least-squares fit.

First, we define an error function G as

$$G(B)=\sum_{i=1}^{M}[\Delta_i^m-\Delta_i^c(B,\phi_i)]^2$$

$$+[\Delta_i^m-\Delta_i^c(B,\phi_i)]^2\ , \qquad (7)$$

where the indices m and c are the experimental and calculated values of the specified items, respectively. Numerical iteration is used to obtain the optical constants and film thickness by minimizing the value of $G(B)$. If the $2M$ sets of equations

$$\sum_{j=1}^{M}\frac{\partial\psi_i}{\partial b_j}\delta b_j=0 \ \text{ and } \ \sum_{j=1}^{M}\frac{\partial\Delta_i}{\partial b_j}\delta b_j=0\ , \qquad (8)$$

where $i=1,\ldots,M$, are linearly independent, then the parameters B can be solved to satisfy the equations

$$\psi_i^m=\psi_i^c(B,\psi_i) \ \text{ and } \ \Delta_i^m=\Delta_i^c(B,\psi_i)\ . \qquad (9)$$

On the other hand, if some of these $2M$ equations are linearly dependent, the number of independent equations is less than the number of unknown parameters, then

$$\frac{\partial\Delta_i^c}{\partial b_j}(B_0,\phi_i)=\text{const}\times\frac{\partial\Delta_j^c}{\partial b_j}(B_0,\phi_i)\ . \qquad (10)$$

Here we neglect the terms $\sum(\partial\psi/\partial b_j)\delta_j$, since in general $\partial\psi/\partial b_j \ll \partial\Delta/\partial b_j$. Equation (10) implies that a change of the incident angle ϕ_i cannot be used to obtain new information about Δ_i^c. In this case, the correlated optical constants cannot be determined by the method of multiple incident angles. Some of the parameters should be measured by other techniques. The linear dependence of the ellipsometry functions should be checked at first, so that one can stop to proceed the elaborate measurements without obtaining useful data.

The schematic arrangement of the multiple-wavelength ellipsometer is shown in Fig. 1. The chopped light of Xe lamps after passing through a monochromator is focused by a set of lenses to give a nearly parallel beam. The polarizer and analyzer are made of dichroic films with an extinction ratio of 1:50 within the visible light. The polarizers are mounted on a divided circle assembly which rotate 360° with a precision of ±0.05°. The quarter-wave plate is an L-135 Gaertner Soleil-Babinet compensator

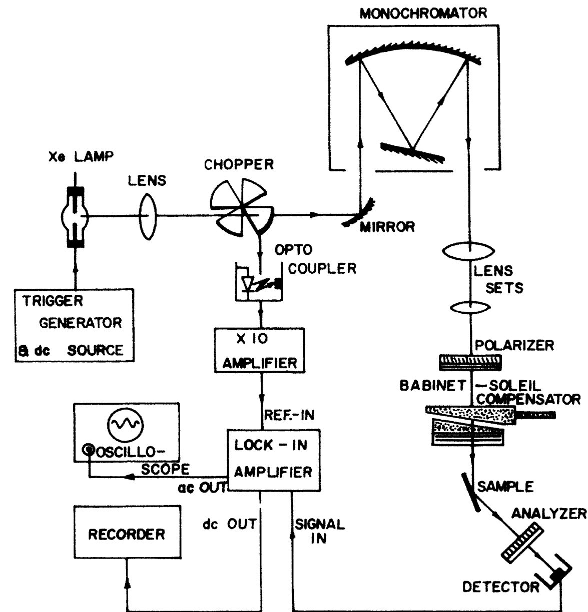

FIG. 1. Schematic construction of the multiple-wavelength ellipsometer.

which is composed of two quarter wedges having their optical axes parallel to their faces and to each other combined with another plane parallel quartz plate and its optical axes perpendicular to the axes of the wedges. The amount of transverse motion is indicated by a micrometer drum divided into 100 parts. Since the light is partially polarized after transmitting through the monochromator, a mica sheet with a thickness of 0.3 mm mounted on a tiltable holder is inserted at the exit of the monochromator for compensating the polarization. The photosignal is detected by an EG&G SGD-100A *p-i-n* photodiode and then demodulated by a Princeton HR-8 lock-in amplifier to enhance the signal-to-noise ratio. The refractive indices of Ni and Si (Ref. 6) measured by this system are checked with the reported data,[7] and the deviation is found to be within 10%.

The precision of the measurement determined by varying repetitively the incident angles with the same sample is better than ±1.71% and ±1.56% for the real and imaginary parts of the refractive index, respectively.

III. SAMPLE PREPARATION

Palladium films of about 400 Å are evaporated by radio-frequency (rf) sputtering onto (100) silicon substrates at room temperature. The wafers purchased from Monsanto were polished to a flatness of $\lambda/20$. The silicides Pd_2Si and PdSi are formed by annealing at temperature of 300 and 800 °C, respectively, for 40 min under an oil-free vacuum system to a pressure below 10^{-6} Torr. The resulting PdSi films are very stable[8] and form polyhexagonal structures as determined by a transmission electron microscope. The depth profiles of the Pd_2Si and PdSi phases have been identified by a Perkin-Elmer PH590 Auger-electron spectrometer (AES) as shown in Figs. 2 and 3, respectively. Since the ion-beam sputtering

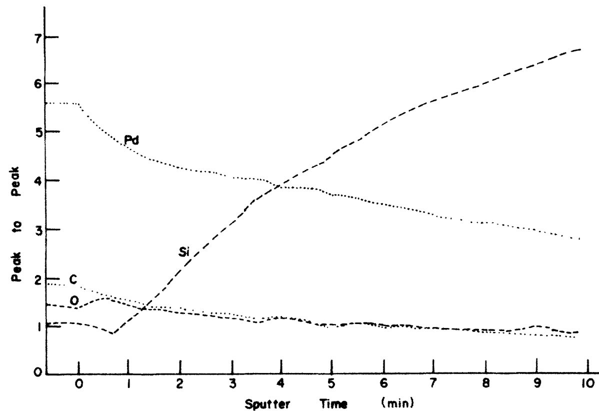

FIG. 2. Peak-to-peak AES depth profile of Pd_2Si. The AES sensitivity factors for Pd and Si are 0.83 and 0.37, respectively. The electron beam energy is 3 keV, argon ion beams of 2 keV, are used for sputtering the surface under a based pressure of 10^{-10} Torr.

during AES profile measurement will introduce local heat to the sample which might be larger than from the annealing process, the relative sensitivities of silicon Auger signals in different compound matrices are still not quite clear, and the AES determination of compound composition cannot be very accurate. The Auger spectrum of the high-temperature annealed PdSi (Fig. 3) will be less influenced by localized heating than that of Pd_2Si and thus gives a better composition identification. The silicon oxide which is grown during annealing is etched by a buffered solution (5% high frequency) (HF) just before the ellipsometry measurement. The samples are rejected if the surfaces show milky reflection or are spotted after annealing. Therefore the effects due to oxides, surface roughness, and contaminants are greatly reduced. Δ and ψ for each sample are measured ten times and averaged for each wavelength.

IV. EXPERIMENTAL RESULTS

The real (n) and imaginary (k) parts of the refractive indices of the as-deposited Pd_2Si and PdSi are shown in Figs. 4, 5, and 6, respectively. It succinctly reveals that the character of k changes from monotonically increasing from Pd_2Si to decreasing for PdSi. The magnitudes of k also show a great reduction from 5 to 1.2 at 700 nm for these two silicides with a consequence of reducing the reflectivity. These results are likely to be due to the change of valence electrons from forming metallic bonds into intermetallic silicide compounds as the annealing temperature increases. The change of the real part n is not so rapid, but indicates the existence of an extremum value near 520 nm for the PdSi which may arise from the interband-electron and phonon interaction with a thermal broadening of the phonon spectrum.

A classical model of a free-electron gas derived by Drude[9] assuming the phase velocity of the incident wave being greater than the Fermi velocity of the electron indicates that the conductivity can be written as

$$\sigma=\frac{e^2}{12\pi^3}\int\frac{\tau_v(1+i\omega\tau)}{1+\omega^2\tau^2}dS_F=\sigma_0\frac{1+i\omega\tau}{1+\omega^2\tau^2}\ , \tag{11}$$

where τ is the electron relaxation time, ω is the incident wave frequency, $\sigma_0=(Ne^2/m)\tau=1/4\pi\omega_p^2\tau$ is the dc conductivity, and ω_p is the plasma frequency. The real and imaginary parts can be derived from

$$n-ik=\left[\epsilon+\frac{4\pi\sigma}{\omega}i\right]^{1/2}\ , \tag{12}$$

and are given by

$$\begin{aligned}\epsilon_1&=n^2-k^2=\epsilon-\frac{\omega_p^2\tau^2}{1+\omega^2\tau^2}\ ,\\ \epsilon_2&=2nk=\omega_p^2\tau/\omega(1+\omega^2\tau^2)\ .\end{aligned} \tag{13}$$

The complex dielectric constant ϵ may differ from 1 by

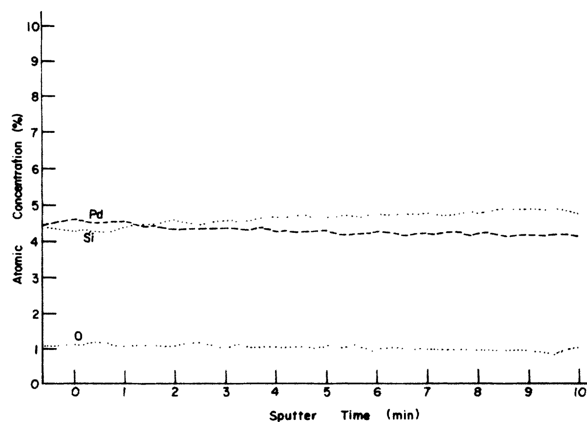

FIG. 3. Direct plot of the atomic concentrations of the AES depth profile of the PdSi.

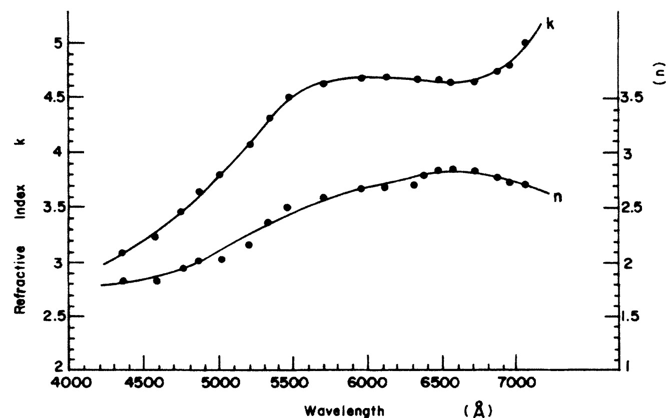

FIG. 4. Real (n) and imaginary (k) parts of the refractive indices for as-deposited Pd at various wavelengths.

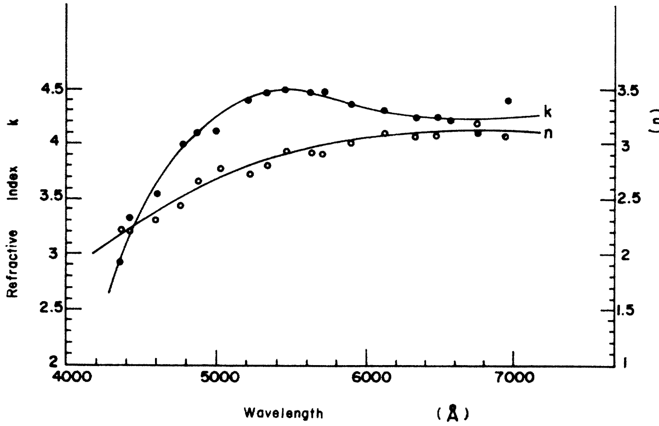

FIG. 5. n and k of Pd_2Si.

$$\epsilon(\omega)=1+\frac{4\pi Ne^2}{m}\sum_j f_j\frac{1}{\omega_j^2-\omega^2}\ , \qquad (14)$$

where ω_j are all the possible resonance transitions with a structure factor f_j. For pure metals, the relaxation time may be smaller than 10^{-14} sec. Thus near the infrared, if $\omega \ll 1/\tau$, we have $|\epsilon_1| \ll |\epsilon_2|$ and $k > n \gg 1$. The reflection and absorption are both high in this classical shin-depth region. In addition to the pure conduction-band transition, the electrons of Pd metal also show the optical transition from the valence $4d$ to conduction band for photon energy being greater than 3.1 eV. The reflectance is high for the whole visible light range with $h\nu < 3.1$ eV and the as-deposited film shows a shiny color. For Pd_2Si, $n \approx k$ within the visible region, but k becomes smaller than n at photon energies greater than 2.95 eV. This intersection point usually occurs at the plasma oscillating frequency which decreases as the density of conduction electrons decreases due to silicide hybridization. On the other hand, the imaginary part k of Pd and PdSi always remains greater than the real part within the uv and visible region therefore is in agreement with the relaxation mechanism.

To study the influence of electronic band structure on the optical reflectivity, an x-ray photoelectron spectrometer (Perkin Elmer PHI1905) is used to study the binding energies of Pd $3d_{5/2}$ and $3d_{3/2}$ core levels. As shown in Fig. 7, the binding energy of Pd $3d_{5/2}$ shift from 335.2 eV for the pure Pd metal, to 336.2 eV for the Pd_2Si and then to 337 eV for the PdSi. The binding energies of electrons are proportional to the attractive force with the nuclear charges and are counterbalanced by the outer valence electrons which exert a repulsive force on the core electrons acting as a screen potential. If an electron is removed from the outer shell, the screening of the inner electrons is reduced by one electron charge, and the core electrons exhibit higher binding energies. On the other hand, if the metals are oxidized, i.e., a gain of an outer electron, it has the opposite effect of increasing the shielding and therefore decreasing the binding energy.

The effective charge of the core electrons contributed from neighbor atoms can be deduced from the electronegativity of the elements[10] as written by

$$\Delta q=\sum_i I_i=\sum_i \frac{\chi_A-\chi_B}{|\chi_A-\chi_B|}[1-e^{-0.25(\chi_A-\chi_B)^2}]\ , \qquad (15)$$

where χ_A and χ_B are the electronegativities, respectively, for the atom under study and its neighbor, and $\sum_i$ is summed over all of the electronic bonds. The chemical shift ΔE_{nl} for the orbital nl between a free atom and a particular molecular state can then be approximated by the Koopmans' theorem, which yields

$$\Delta E_B = e^2\Delta q/\langle \gamma_B\rangle_{nl}\ , \qquad (16)$$

where $\langle \gamma_B\rangle_{nl}$ is the average Bohr radius. For PdSi compounds, we have $\chi(\mathrm{Si})=1.95$ eV, $\chi(\mathrm{Pd})=2.2$ eV, $\sum_i=2$, and $e^2/\langle \gamma_B\rangle_{3d_{5/2}} \approx 39$ eV. The calculated $\Delta E_B \approx 1.2$ eV is very close to the experimental value as given by 1.8 eV. Examining the binding energy of the Si $2p$ orbital which only shifts slightly from 99.15 eV for a clean Si surface to 99.6 eV for the silicide clearly indicates the charge

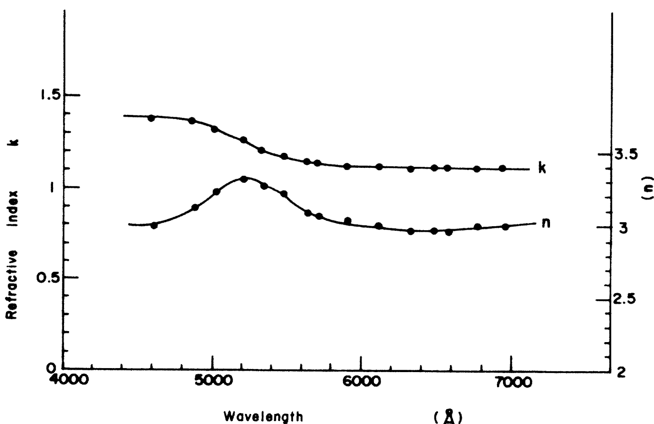

FIG. 6. n and k of PdSi.

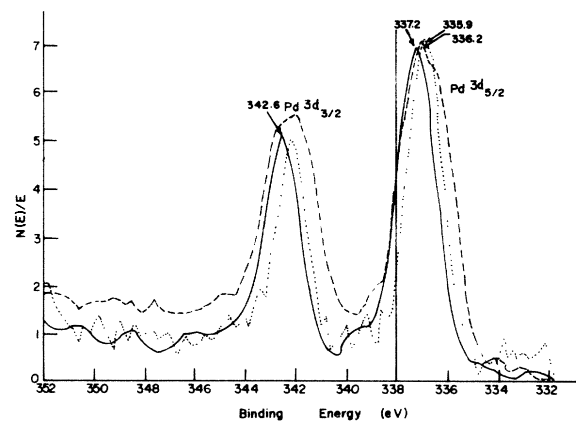

FIG. 7. Binding energy of Pd $3d_{5/2}$ and $3d_{3/2}$ as measured by XPS. The Al $K\alpha$ x rays were used with an analyze scan range of 1000—0 eV.

transfer from Pd to Si.[11] Since silicides are intermetallic compounds, the conductivity of silicides decreases as the temperature increases resulting from the hybridization of the $4d$ electrons of Pd with the valence $3p$ electrons of Si and empty $3d$ orbitals of Si. The resistivities measured by four-point probes are 10.8, 20, and 35 $\mu\Omega$ cm for the as-deposited Pd, Pd_2Si, and PdSi, respectively, which clearly confirms this result. The decrease of conductivity presumably increases $\epsilon_1(=1-4\pi\sigma\tau<0)$ and decreases $\epsilon_f(=4\pi\sigma/\omega>0)$ and k is likely to approach n, the silicides have a lower reflectivity than pure Pd within the visible light.

V. CONCLUSIONS

Optical properties and electronic band structures of silicides need further exploration for device modeling. The optical refractive indices change rapidly from phase to phase in a very complex manner at different growth temperatures. The optical absorption and dispersion of silicides may be controlled mainly by conduction-electron absorption for the pure transition metals and then by valence and core electron absorption through interband and intraband transitions for high-temperature annealed silicides.

ACKNOWLEDGMENT

This work was supported by the National Science Council at the Republic of China under Contract No. NSC 75-0608-M007-01.

[1]J. T. Lue, Solid-State Electron. **26**, 787 (1983).

[2]H. Elabd and W. F. Kosonocky, RCA Rev. **43**, 568 (1982).

[3]J. M. Pimbly and W. Katz, Appl. Phys. Lett. **42**, 984 (1983).

[4]S.Y. Shaw and J. T. Lue, J. Phys. E **14**, 1135 (1981).

[5]R. M. A. Azzam and N. M. Bashara, *Ellipsometry and Polarized Light,* 1st ed. (North-Holland, Amsterdam, 1977).

[6]H. W. Chen and J. T. Lue, J. Appl. Phys. **59**, 2165 (1986).

[7]D. W. Lynch and W. R. Hunter, *Handbook of Optical Constants of Solids,* edited by E. D. Palik (Academic, New York, 1985), p. 317.

[8]K. N. Tu and J. W. Mayer, *Thin Films—Interdiffusion and Reactions,* edited by J. M. Poate, K. N. Tu, and J. W. Mayer (Wiley, New York, 1978), pp. 359–404.

[9]J. N. Hodgson, *Optical Absorption and Dispersion in Solids* (Chapman and Hall, London, 1970), pp. 64–65.

[10]T. A. Carlson, *Photoelectron and Auger Spectroscopy* (Plenum, New York, 1975), Chap. 5.

[11]P. J. Grunthaner, F. J. Grunthaner, A. Madhukar, and J. W. Mayer, J. Vac. Sci. Technol. **19**, 649 (1981).